

Supporting Information

Studies on the Claisen Rearrangements in the Indolo[2,3-*b*]quinoline System

Nicholas Voûte, Douglas Philp, Alexandra M.Z. Slawin and Nicholas J. Westwood*

School of Chemistry and Biomolecular Sciences Research Complex, University of St Andrews, North Haugh, St Andrews, KY16 9ST, UK.

***Correspondence author: Tel.: +44-1334-463816; fax: +44-1334-463808;
email: njw3@st-andrews.ac.uk**

Page S1	Contents.
Page S2	Attempted Claisen rearrangement of 1 : Kinetic studies.
Page S2-3	Attempted Claisen rearrangement of 1 : NMR analysis.
Page S3-5	Computational studies for the Claisen and aza-Cope rearrangement of 1 and 2 .
Page S5-6	Autoxidation of 21 .
Page S6-7	Determination of the enantiomeric ratio of (S)-(+)-3-buten-2-ol.
Page S7-8	Determination of the enantiomeric ratio of 18 .
Page S8-10	An alternative synthesis of 20 .
Page S11-24	¹ H and ¹³ C NMR spectra.
Page S25	References.

Supporting Information

Attempted Claisen rearrangement of **1**: Kinetic studies

When **1** was rearranged to **6** at a range of starting concentrations no change in rate was observed (**Table S1**). This suggested that the reaction followed first order kinetics consistent with an intramolecular tandem Claisen-aza-Cope processes.

Rearrangement of 1 to 6 in refluxing toluene	
Concentration of 1 (mol dm ⁻³)	6 : 1 after 12 hours*
0.25	34:66
0.05	37:63
0.01	37:63

* Calculated from integration of CH₃ peaks in the crude ¹H NMR spectrum.

Table S1. The effect of concentration on the rate of O-11 to N-5 allyl migration in **1**.

Attempted Claisen rearrangement of **1**: NMR analysis

Whilst the kinetic studies described above are consistent with an intramolecular tandem Claisen-aza-Cope processes, it was decided to assess the transformation of **1** to **6** using ¹H and 2D ¹H-¹³C HMBC NMR techniques in an attempt to observe the proposed intermediate **5**. Generally, the intermediate species in two step consecutive reactions reaches the highest concentration early in the reaction progress. Based on this assumption, it was reasoned that detection of **5** would be most likely early in the reaction before large amounts of **1** had been consumed. After heating **1** for one hour at 100 °C, detailed analysis of the ¹H NMR spectrum associated with the crude reaction mixture indicated the presence of a trace quantity (approximately 0.5% in comparison to **1**) of a third compound that was neither **1** nor **6** (**Figure S1**). It was reasoned that if this additional compound was **5** it should be possible to detect a signal for C-11 of the carbonyl group at approximately 200 ppm in the ¹³C NMR spectrum. Due to the low concentration of this compound in relation to **1** the sensitive HMBC experiment was used. Indeed, this analysis did indicate the presence of a carbon with a chemical shift of 195 ppm that correlated with a signal at 8.00 ppm in the ¹H dimension, presumed to be H-1 of **5**. Not only did this give further support to the proposed intermediacy of **5**, it also demonstrated that **5** was a relatively stable and long lived species.

Supporting Information

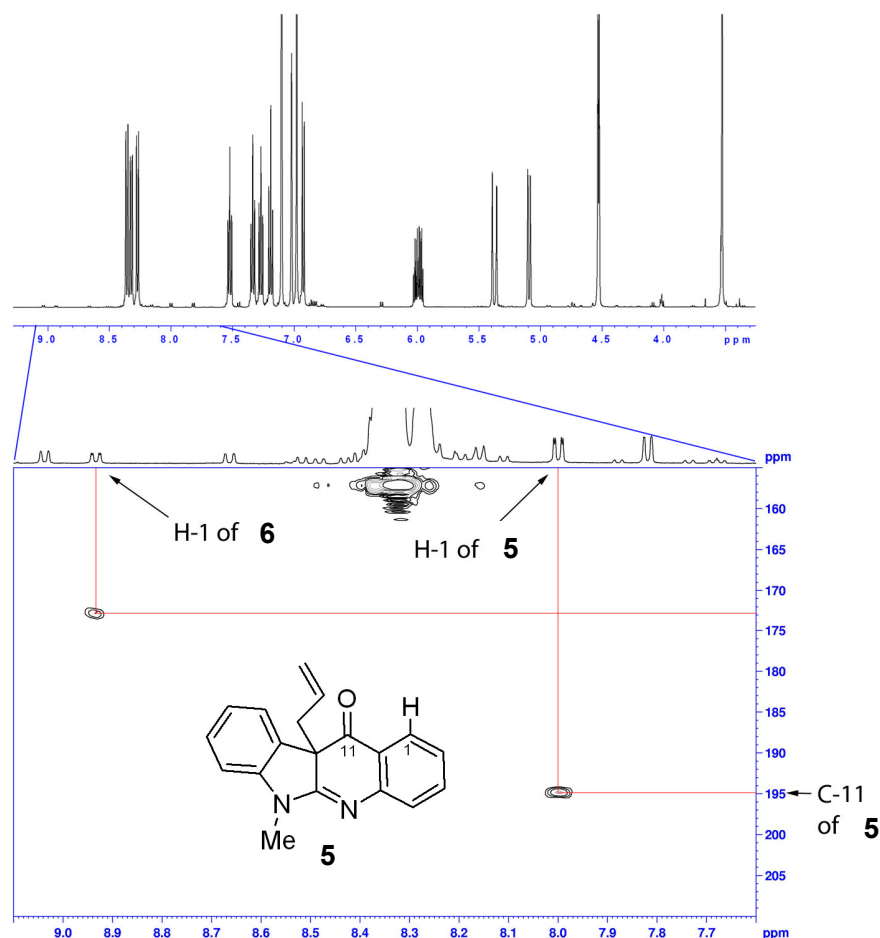


Figure S1. After heating **1** in toluene- d_8 for one hour, ^1H NMR and $^1\text{H}^{13}\text{C}$ HMBC spectra indicate the presence of **5**. The major peaks in the ^1H dimension correspond to the protons of **1**.

Computational studies for the Claisen and aza-Cope rearrangement of **1** and **2**

In order to better understand the differences in chemical behaviour between the two systems **1** and **2** the rearrangement sequences for both compounds were investigated computationally using the procedure described below.

Initially, the lowest energy conformations of **1**, **5**, **6** were located using molecular mechanics calculations using the MMFF forcefield as implemented in Macromodel (Version 9.5, Schrödinger Inc., 2007). The structures of the lowest energy conformations of the ground states of **1**, **5**, **6** were then refined using the AM1 semi-empirical method and the appropriate lowest energy conformations, located for each compound, were used to generate guess structures for the transition states linking **1** and **5** and **5** and **6** using the linear synchronous transit method. The guess transition states were then

Supporting Information

refined using the eigenvector following method at the AM1 level of theory using MOPAC2007^{S1} to stationary points that possessed one imaginary vibration. These crude TS guesses were then used as input structures for the DFT calculations using the B3LYP functional and a 6-31G(d,p) basis set. Electronic structure calculations were carried out using GAMESS^{S2} running on a Linux cluster. The 64-bit Linux version dated 24 Mar 2007 (Revision 6) was used in all calculations. All of the transition states located for the two rearrangements have the classical chair-like structure. Vibrational frequency analysis and intrinsic reaction coordinate (IRC) calculations verified that all of the transition state structures located were valid and energies for each species on the reaction pathways were extracted by standard methods.

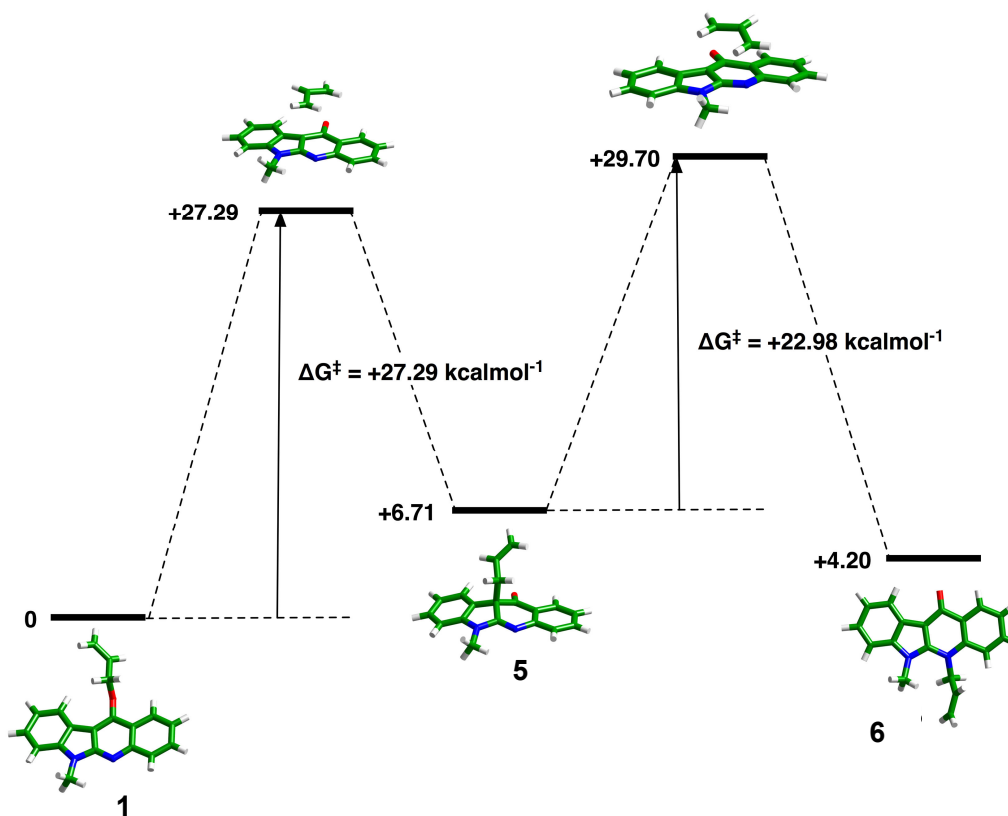


Figure S2. Calculated energy barriers (B3LYP/6-31G(d,p)) for the conversion of **1** to **5** and the conversion of **5** to **6**. The transition state geometries are shown and adopt the classic chair-like structure.

The reaction sequence **2** to **7** to **8** was also investigated at the B3LYP/6-31G(d,p) level of theory using the methodology outlined above. As before, all of the transition states located for the two rearrangements have the classical chair-like structure and vibrational frequency analysis and intrinsic

Supporting Information

reaction coordinate (IRC) calculations verified that all of the transition state structures located were valid and energies for each species on the reaction pathways were extracted by standard methods.

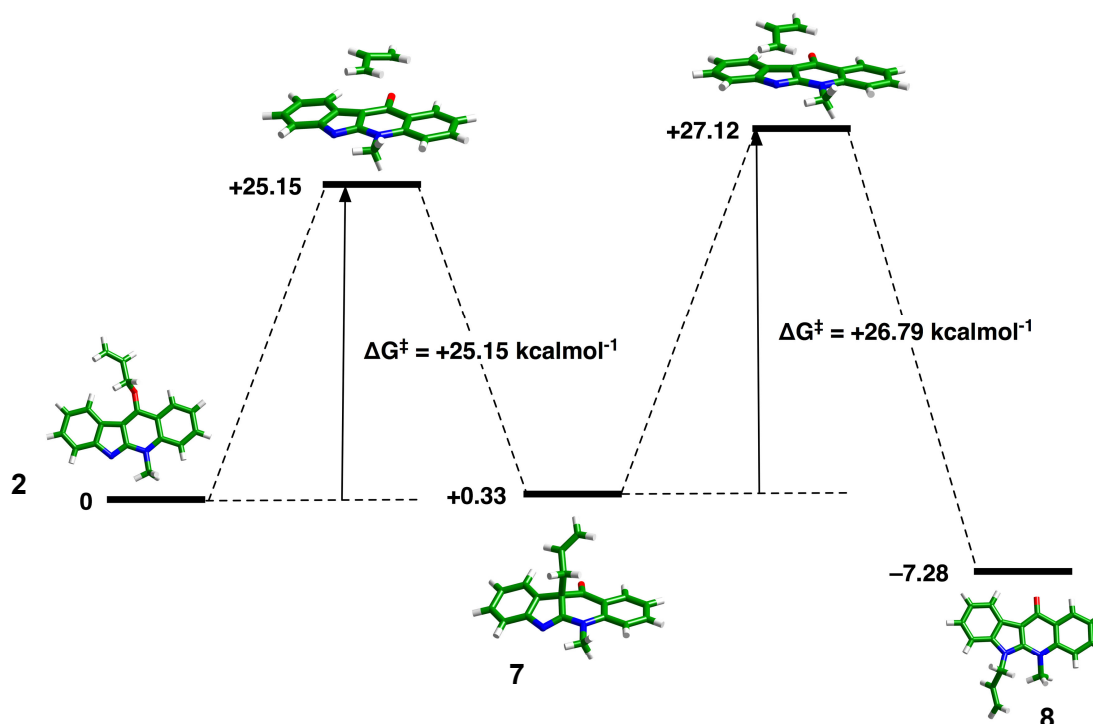
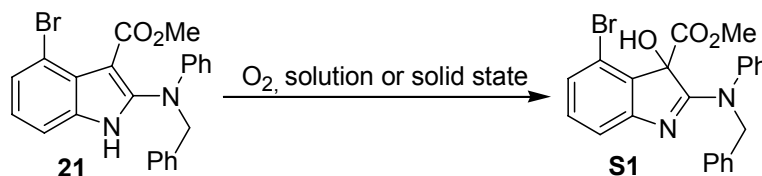


Figure S3. Calculated energy barriers (B3LYP/6-31G(d,p)) for the conversion of **2** to **7** and the conversion of **7** to **8**. The transition state geometries are shown and adopt the classic chair-like structure.

Autoxidation of **21**

A further complication related to the synthesis of **21** arose from the propensity of **21** to undergo a rapid autoxidation to **S1** (**Scheme S1**). In less than five days a complete and clean transformation of **21** to **S1** was observed in either the solid state or in solution.

Supporting Information

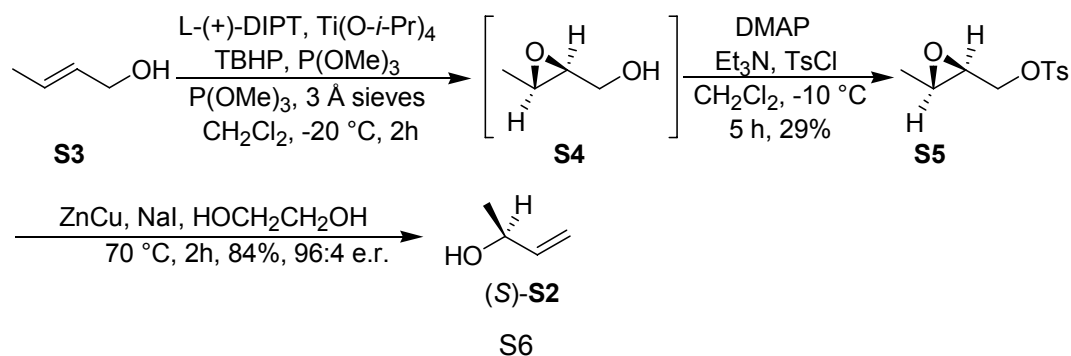


Scheme S1. 2-Aminoindole **21** was found to undergo a rapid autoxidation to **S1**.

Spectroscopic characterisation for **S1** was as follows: Colourless crystalline solid. Mp 156-158 °C; IR (KBr) ν_{max} : 3478 (br m, O-H), 1747 (s, C=O), 1558 (s), 1496 (m), 1454 (m), 1430 (s), 1249 (s), 1167 (m), 1103 (m), 1018 (w), 946 (w), 905 (w), 782 (m), 753 (w), 700 (m), 515 (w) cm^{-1} ; MS (CI) m/z 451 ($^{79}\text{BrMH}^+$, 100), 453 ($^{81}\text{BrMH}^+$, 85); HRMS (CI) m/z calcd for $\text{C}_{23}\text{H}_{20}\text{N}_2\text{O}_3^{79}\text{Br}$ 451.0657, found 451.0652; ^1H NMR (300 MHz, CDCl_3) δ 7.04-7.37 (m, 12H, 12 x ArH), 6.98 (dd, $J = 7.5, 1.5$ Hz, 1H, ArH), 5.28 (d, $J = 14.5$ Hz, 1H, CH_2), 4.97 (d, $J = 14.5$ Hz, 1H, CH_2), 3.72 (s, 1H, OH), 3.60 (s, 3H, CH_3); ^{13}C NMR (75 MHz, CDCl_3) δ 170.5 (C, C=O), 169.7 (C, C-2), 158.4 (C), 140.3 (C), 136.7 (C), 134.0 (C), 132.2 (CH), 130.1 (CH), 129.0 (2 x CH), 128.9 (4 x CH), 128.6 (2 x CH), 127.8 (CH), 125.9 (CH), 116.9 (C), 116.6 (CH), 84.0 (C, C-3), 57.2 (CH_2), 53.9 (CH_3).

Determination of the enantiomeric ratio of (S)-(+)-3-buten-2-ol

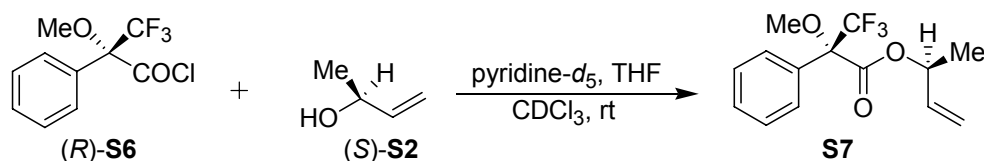
Enantiomerically enriched (S)-(+)-3-buten-2-ol (**S2**) was synthesised using literature procedures starting from *trans*-2-butene-1-ol (**S3**) (**Scheme S2**).^{S3,S4} Sharpless asymmetric epoxidation of **S3** with *tert*-butyl hydroperoxide (TBHP), in the presence of L-(+)-diisopropyl tartrate (DIPT), followed by the *in situ* tosylation of the resulting epoxide **S4** afforded (2S,3S)-(-)-epoxytosylate **S5** in high chemical and optical purity after repeated crystallisation in accordance with the literature precedent.^{S3} The optical purity of **S5** synthesised by this method was assessed by comparison of the optical rotation with a literature value. It is reported that the (2R,3R)-(-)-enantiomer of **S5** with an enantiomeric purity of >99:1 e.r., determined by ^1H NMR analysis in combination with a chiral shift reagent, has an optical rotation of $[\alpha]^{25}_{\text{D}} = +34.2$.^{S3} The optical rotation of (2S,3S)-**S5** was recorded to be $[\alpha]^{20}_{\text{D}} = -38.6$ suggesting that the optical purity of (2S,3S)-(-)-**S5** was also of >99:1 e.r.



Supporting Information

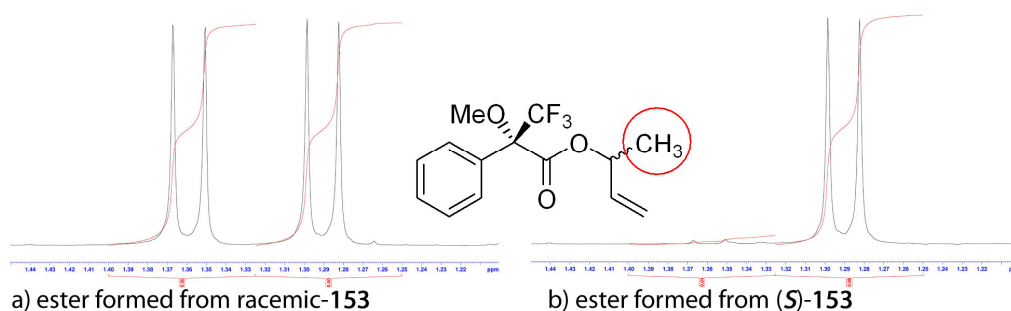
Scheme S2. Synthesis of enantiomerically enriched (S)-(+)-3-butene-2-ol. DIPT = diisopropyl tartrate, TBHP = *tert*-butyl hydroperoxide, DMAP = 4-dimethylaminopyridine, Ts = *p*-toluenesulfonyl.

Treatment of **S5** with sodium iodide and zinc-copper couple in ethylene glycol led to the formation of (S)-**S2** in good yield.^{S4} Due to the volatility of (S)-**S2**, ethylene glycol was used as the solvent in this reaction and the product was separated by distillation at atmospheric pressure. By stirring a tetrahydrofuran solution of (S)-**S2** with 3 Å molecular sieves, the water that had co-distilled with (S)-**S2** was removed. However, the tetrahydrofuran could not be separated from the volatile (S)-**S2** and in subsequent reactions (S)-**S2** was used as a solution in tetrahydrofuran. The concentration of (S)-**S2** in tetrahydrofuran was determined by analysis of the ¹H NMR spectrum associated with this tetrahydrofuran solution and was found to be *ca.* 2.7 M. The enantiomeric purity of (S)-**S2** was determined by formation of an ester of (S)-**S2** with the chiral derivatising reagent (*R*)-(-)- α -methoxy- α -(trifluoromethyl)phenylacetyl chloride ((*R*)-MTPACl, (*R*)-**S6**) (**Scheme S3**).^{S5}



Scheme S3. Determination of enantiomeric purity of (S)-**S2** by the formation of an ester with (*R*)-(-)- α -methoxy- α -(trifluoromethyl)phenylacetyl chloride.

Using ¹H NMR, the diastereoisomeric composition of **S7**, which is related to the enantiomeric composition of (S)-**S2**, was determined by integration of the methyl doublet in **S7** that showed a large chemical shift non-equivalence (**Figure S4**). Using this method it was found that (S)-**S2** had been formed with an enantiomeric purity of 96:4 e.r. For comparison, this derivatisation and ¹H NMR analysis was also conducted on commercially available racemic-**S2**, using identical reaction conditions. This showed the expected 1:1 ratio of diastereoisomers, suggesting that under these conditions a kinetic resolution had not taken place.



Supporting Information

Figure S4. Analysis of the MTPA esters formed from a) racemic-**S2** and b) (S)-**S2** by ^1H NMR demonstrated that (S)-**S2** had been formed in 96:4 e.r.

Determination of the enantiomeric purity of **18**

The enantiomeric purity of **18** was determined using the chiral lanthanide shift reagent $\text{Eu}(\text{hfc})_3$ (hfc = heptafluorohydroxymethylene-(+)-camphorato) (**Figure S5**).^{S6} The addition of $\text{Eu}(\text{hfc})_3$ in small portions to **18** in CDCl_3 led to a good separation of the signal in the ^1H NMR spectrum associated with H-1 of **18**. The enantiomeric purity of **18** was measured by integration of these separated signals and was determined to be 93:7 e.r. It must be noted, however, that enantiomeric ratios determined using lanthanide chiral shift reagents have been reported to be most accurate in the region of 70:30 e.r. to 80:20 e.r. with significant errors reported above these values.^{S7} Attempts were made to determine the enantiomeric purity of **18** with greater accuracy using chiral HPLC. Unfortunately, using a variety of solvent systems in combination with both normal and reversed phase columns, the two enantiomers could not be satisfactorily separated.

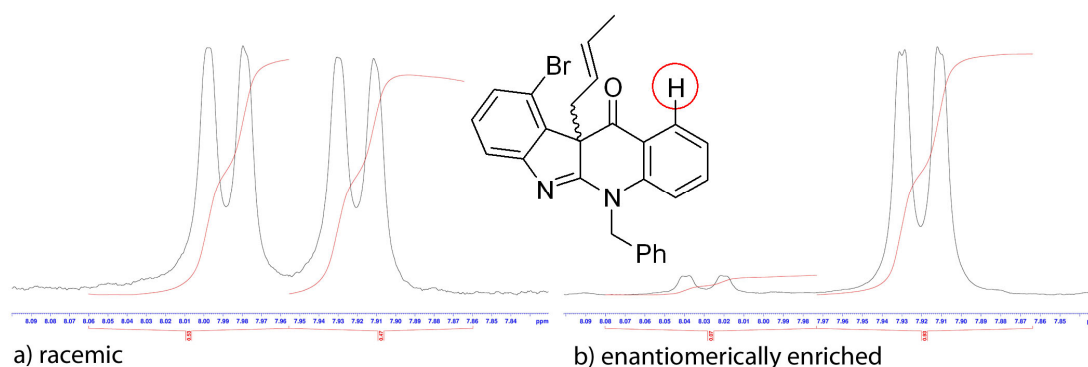
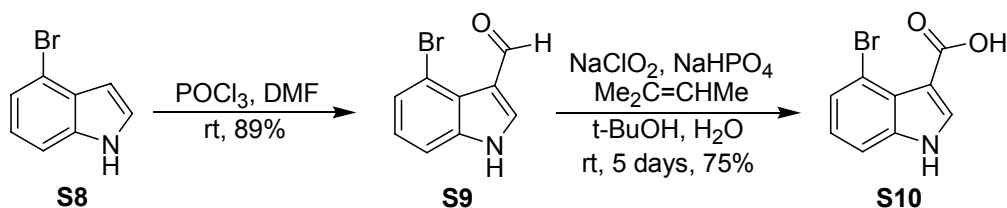


Figure S5. Analysis of a) racemic-**18** and b) enantiomerically enriched **18** using the chiral lanthanide shift reagent $\text{Eu}(\text{hfc})_3$ in combination with ^1H NMR demonstrated that the enantiomeric purity of **18** was 93:7 e.r.

An alternative synthesis of **20**

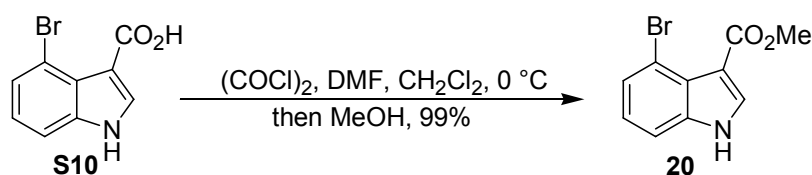
As a synthesis that allowed multigram preparation of **20** was required, a three step protocol involving formylation, oxidation and esterification starting from 4-bromoindole (**S8**) was considered. Utilising the Vilsmeier-Haack reaction, **S8** was converted to the known aldehyde **S9**^{S7} in good yield (**Scheme S3**).

Supporting Information



Scheme S3. Formylation of 4-bromoindole and subsequent oxidation. DMF = *N,N*-dimethylformamide.

The oxidation of **S9** to **S10** using sodium chlorite in the presence of 2-methyl-2-butene^{S8} is reported in the literature but no preparation, isolation, purification or spectroscopic data is reported.^{S7} Nonetheless, it was eventually found that the transformation of **S9** to **S10** required a large excess of reagents and a reaction time of five days at room temperature. Purification of **S10** was achieved by extracting an intensely blue impurity from an aqueous solution of **S10** at high pH with dichloromethane, followed by the addition of aqueous hydrochloric acid to precipitate **S10** of sufficient purity for the subsequent transformation. A revised reaction procedure led to a much higher yielding conversion of **S10** was converted to **20** in nearly quantitative yield on treatment with oxalyl chloride followed by methanol, without isolation of the intermediate acid chloride (**Scheme S4**).



Scheme S4. High yielding esterification using oxalyl chloride and methanol. DMF = *N,N*-dimethylformamide.

Preparation of 4-bromo-1H-indole-3-carbaldehyde (**S9**)

A solution of 4-Bromoindole (5.00 g, 25.5 mmol) in DMF (10 ml) was added dropwise to a stirred mixture of POCl_3 (5.9 ml, 63.3 mmol) and DMF (10 ml). The temperature of the reaction mixture was maintained at $35\text{--}40\text{ }^\circ\text{C}$ for 45 min and then the reaction mixture was added to ice (ca. 50 g) and water (100 ml). NaOH (13 g) in water (60 ml) was added over a period of 0.5 hours. The mixture was boiled for 5 min and then cooled rapidly to $50\text{ }^\circ\text{C}$. The product was collected by filtration and washed with water to afford the title compound **S9** as colourless crystals (5.07 g, 22.6 mmol, 89%). Spectroscopic data was in accordance with that published in the literature.^{S7} Mp $182\text{--}185\text{ }^\circ\text{C}$ (lit.^{S7} $185\text{--}187\text{ }^\circ\text{C}$); ^1H NMR (400 MHz, CDCl_3) δ 10.93 (s, 1H, CHO), 9.32 (br, s, 1H, NH), 8.12 (d, $J = 3.3$ Hz, 1H, H-2), 7.51 (dd, $J = 8.0, 0.9$ Hz, 1H, H-5/H-7), 7.46 (dd, $J = 8.0, 0.9$ Hz, 1H, H-5/H-7), 7.16 (t, $J = 8.0, 1\text{H}$ Hz, H-6).

Preparation of 4-bromo-1H-indole-3-carboxylic acid (**S10**)

Supporting Information

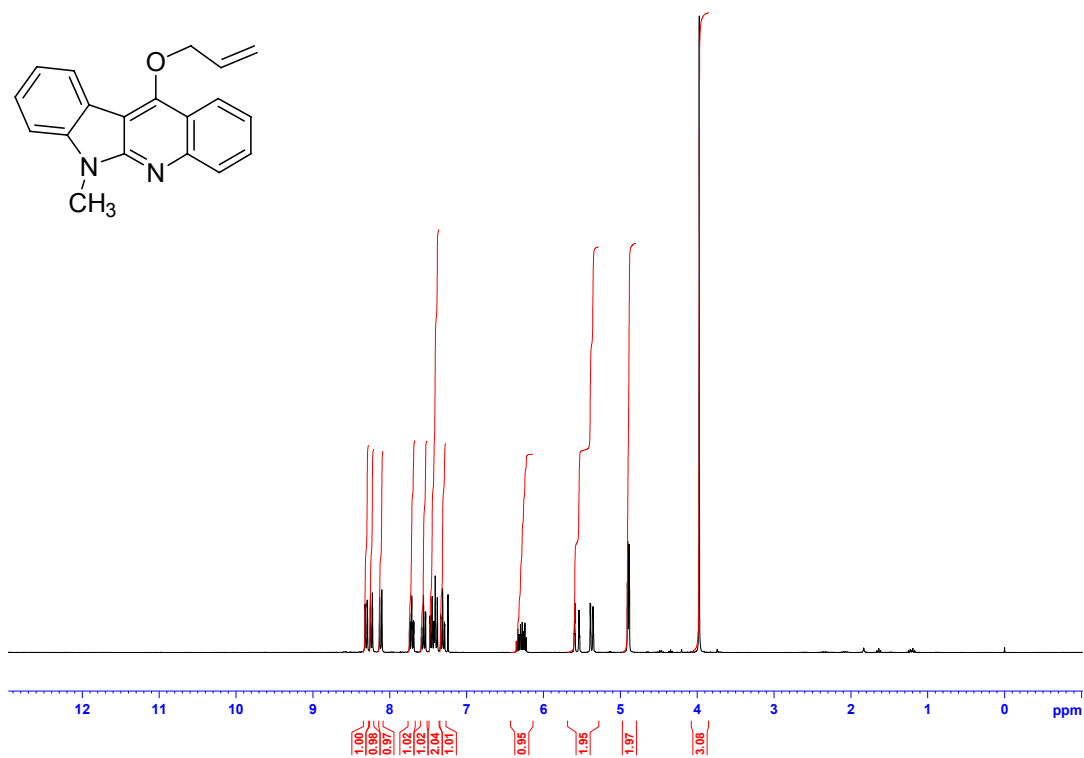
A solution of NaClO₂ (24.2 g, 268 mmol) and NaHPO₄·H₂O (41.9g, 304 mmol) in water (320 ml) was added to a mixture of 4-bromo-1*H*-indole-3-carbaldehyde (**S9**) (4.00 g, 17.9 mmol), 2-methyl-2-butene (47.0 ml, 444 mmol) and *t*-BuOH (200 ml). The reaction mixture was vigorously stirred for 5 days. The *t*-BuOH was evaporated at reduced pressure and, after the addition of water (200 ml), the aqueous residue was extracted with EtOAc (4 x 80 ml). The combined EtOAc extracts were washed with brine (100 ml) and then the EtOAc was evaporated at reduced pressure. The residue was dissolved in 0.5 M NaOH_(aq) (300 ml) and the resulting basic solution was repeatedly extracted with CH₂Cl₂ (ca. 10 x 50 ml) until the aqueous phase was no longer blue. After filtering the aqueous solution through celite, concentrated hydrochloric acid was added to the filtrate until the solution was acidic (ca. pH 5) and the product had crystallised. The product was collected by filtration and washed with water to afford the title compound **S10** as a tan crystalline solid (3.20 g, 13.3 mmol, 75%). Mp 189-190 °C (dec.); IR (KBr) ν_{max} : 3371 (s, N-H), 2931 (br m, O-H), 1675 (s), 1563 (w), 1517 (m), 1447 (m), 1425 (m), 1355 (w), 1329 (w), 1307 (m), 1256 (w), 1192 (m), 1143 (w), 1021 (w), 910 (w), 764 (m), 730 (w), 653 (w), 612 (w), 566 (w) cm⁻¹; MS (EI) *m/z* 241 (⁸¹BrM⁺, 15), 239 (⁷⁹BrM⁺, 15), 197 (90), 195 (100), 116 (49); HRMS (EI) *m/z* calcd for C₉H₆NO₂⁷⁹Br 238.9582, found 238.9584; ¹H NMR (400 MHz, (CD₃)₂CO) δ 11.49 (br, s, 1H, NH/OH), 11.20 (br, s, 1H, NH/OH), 8.06 (d, *J* = 3.0 Hz, 1H, H-2), 7.53 (dd, *J* = 8.0, 0.9 Hz, 1H, H-5/H-7), 7.39 (dd, *J* = 8.0, 0.9 Hz, 1H, H-5/H-7), 7.09 (t, *J* = 8.0 Hz, 1H, H-6); ¹³C NMR (101 MHz, (CD₃)₂CO) δ 164.9 (C), 139.3 (C), 134.6 (CH), 127.5 (CH), 125.7 (C), 124.4 (CH), 114.3 (C), 112.4 (CH), 109.5 (C).

Preparation of 4-bromo-1*H*-indole-3-carboxylic acid methyl ester (**20**)

A mixture of 4-bromo-1*H*-indole-3-carboxylic acid (**S10**) (1.10 g, 4.58 mmol) and oxalyl chloride (0.48 ml, 5.50 mmol) in CH₂Cl₂ (25 ml) was cooled to 0 °C, under an argon atmosphere. DMF (0.35 ml, 4.52 mmol) was added over a period of 0.5 hours. After 1.5 hours, when effervescence had ceased, MeOH (5 ml, 123 mmol) was added and the reaction mixture was allowed to warm to room temperature. Water (40 ml) was added and the mixture was made basic (pH 10) by the addition of 15% NaOH_(aq). The CH₂Cl₂ was separated and the aqueous phase was extracted with CH₂Cl₂ (2 x 20 ml). The combined CH₂Cl₂ extracts were washed with 0.5 M NaOH (20 ml), brine (20 ml) and dried (MgSO₄). Removal of the solvent afforded the title compound **20** as a tan solid of sufficient purity for subsequent reactions (1.15 g, 4.53 mmol, 99%). Spectroscopic data was in accordance with that published in the literature.^{S7} Mp 123-124 °C (lit.^{S7} 125-126 °C); ¹H NMR (400 MHz, CDCl₃) δ 8.93 (br, s, 1H, NH), 7.89 (d, *J* = 3.1 Hz, 1H, H-2), 7.48 (dd, *J* = 8.0, 0.8 Hz, 1H, H-5/H-7), 7.37 (dd, *J* = 8.0, 0.8 Hz, 1H, H-5/H-7), 7.09 (t, *J* = 8.0, 8.0 Hz, 1H, H-6), 3.91 (s, 3H, CH₃).

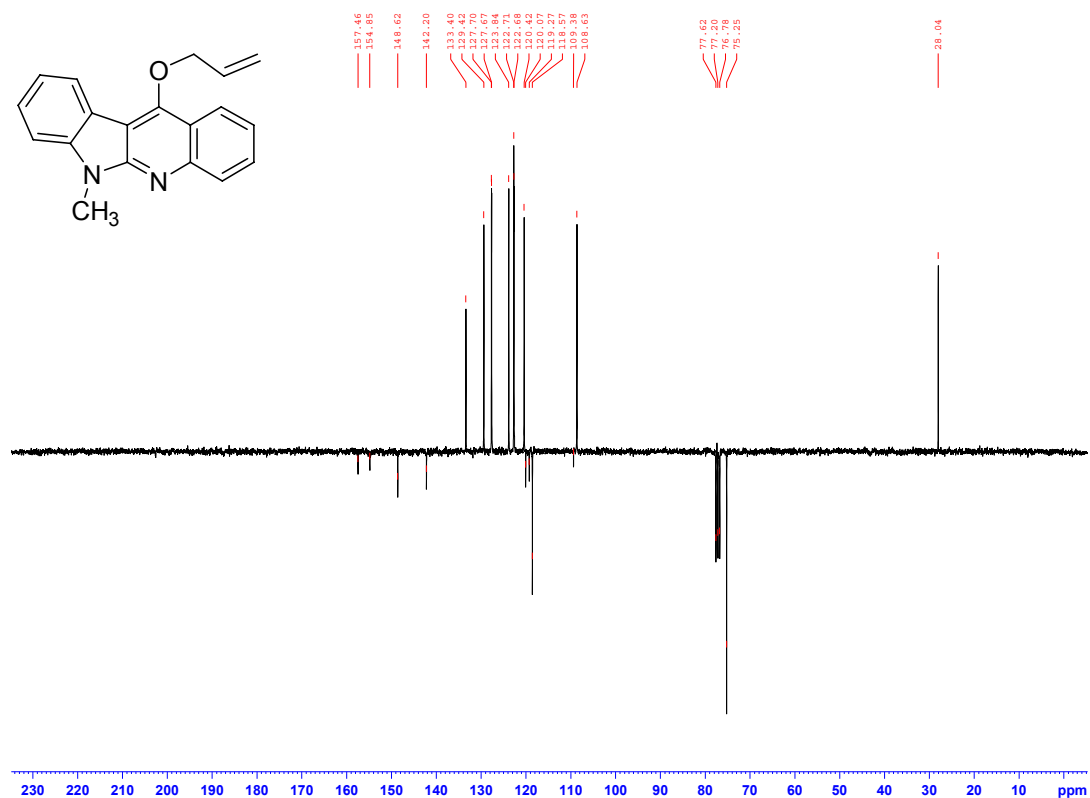
Supporting Information

11-allyloxy-6-methyl-6*H*-indolo[2,3-*b*]quinoline (1) ¹H NMR in CDCl₃



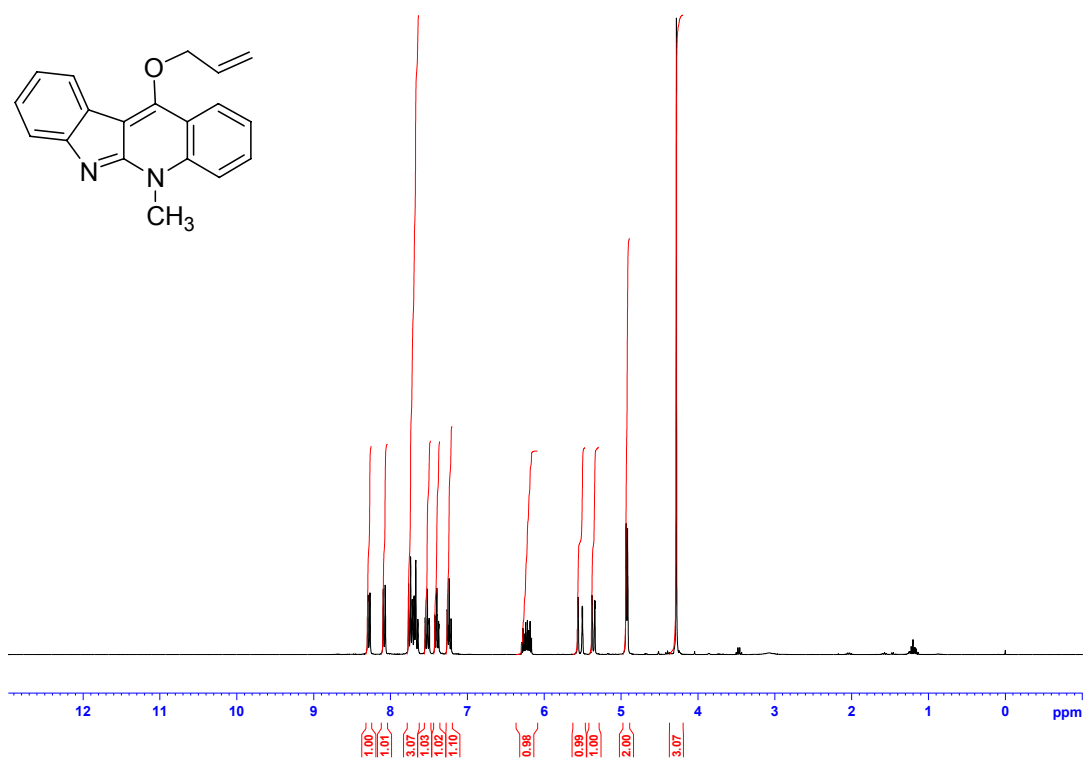
Supporting Information

11-allyloxy-6-methyl-6*H*-indolo[2,3-*b*]quinoline (1) ^{13}C NMR in CDCl_3

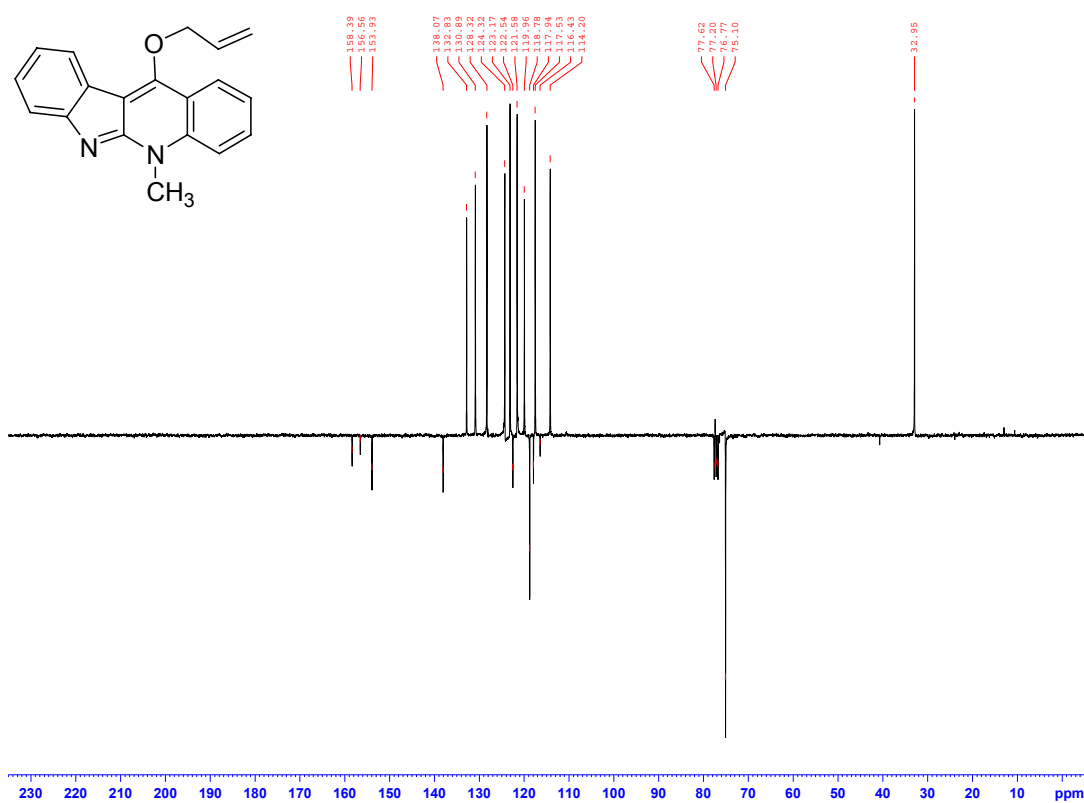


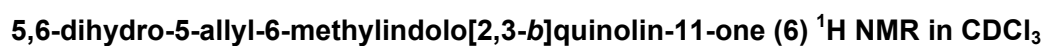
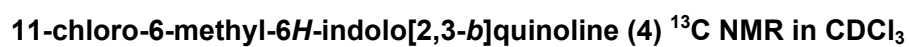
Supporting Information

11-allyloxy-5-methyl-5H-indolo[2,3-b]quinoline (2) ¹H NMR in CDCl₃

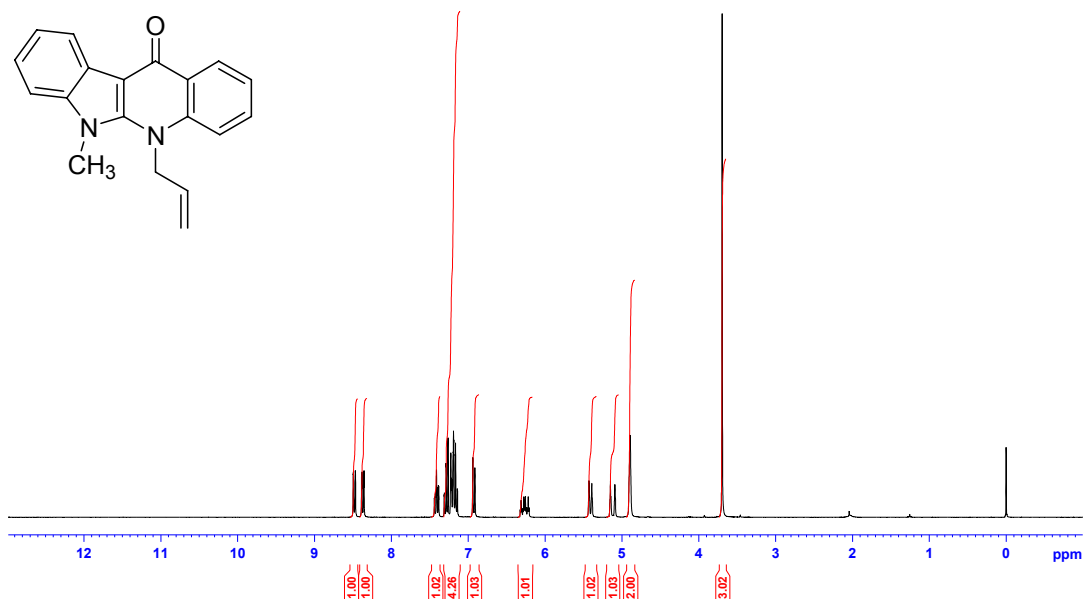


11-allyloxy-5-methyl-5H-indolo[2,3-b]quinoline (2) ¹³C NMR in CDCl₃

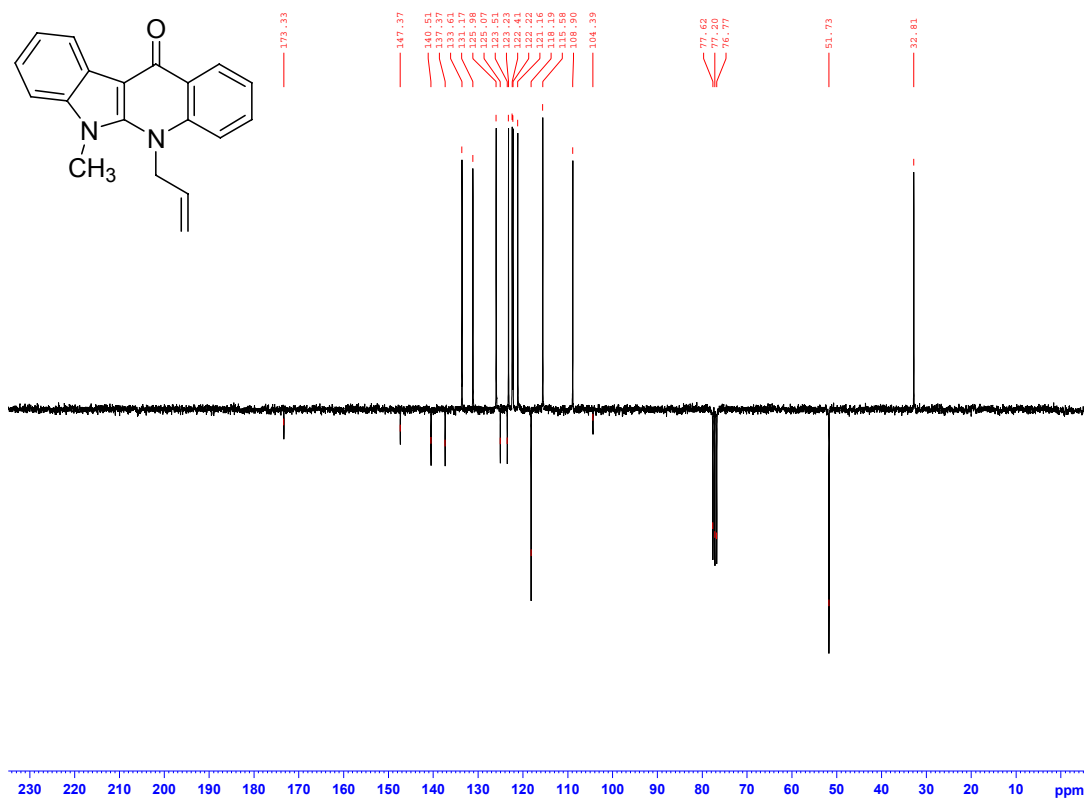


CN1c2ccccc2c3c1c(Cl)ccc3

Supporting Information

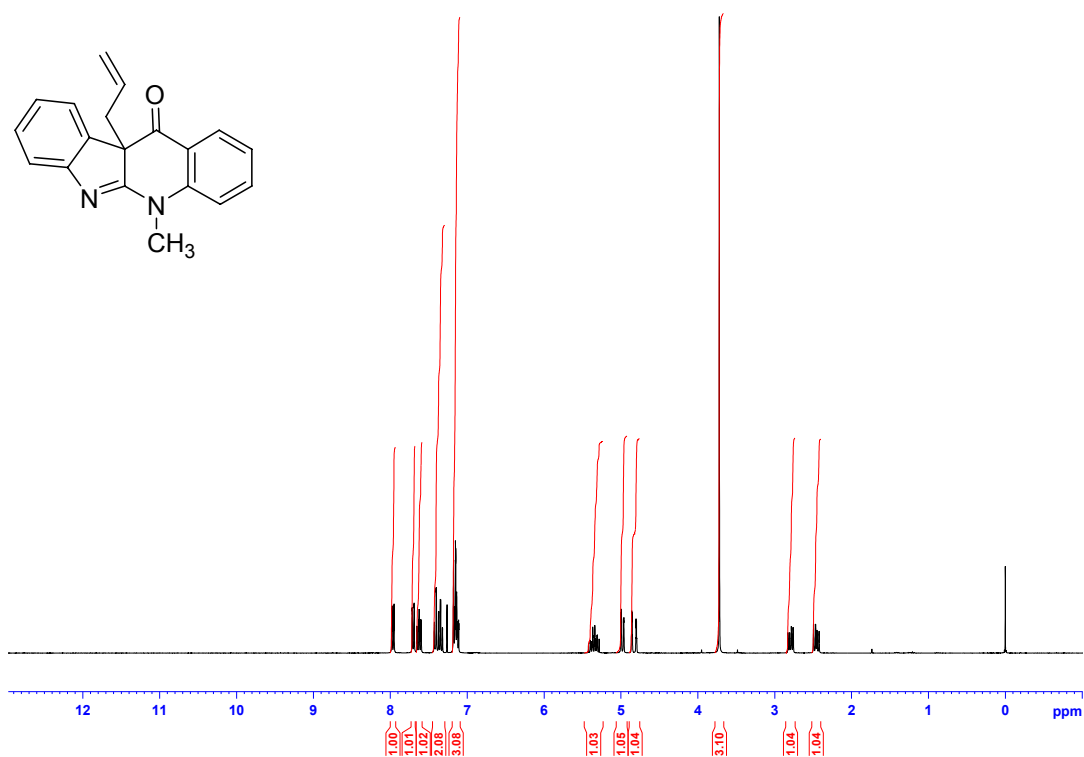


5,6-dihydro-5-allyl-6-methylindolo[2,3-*b*]quinolin-11-one (6) ¹³C NMR in CDCl₃

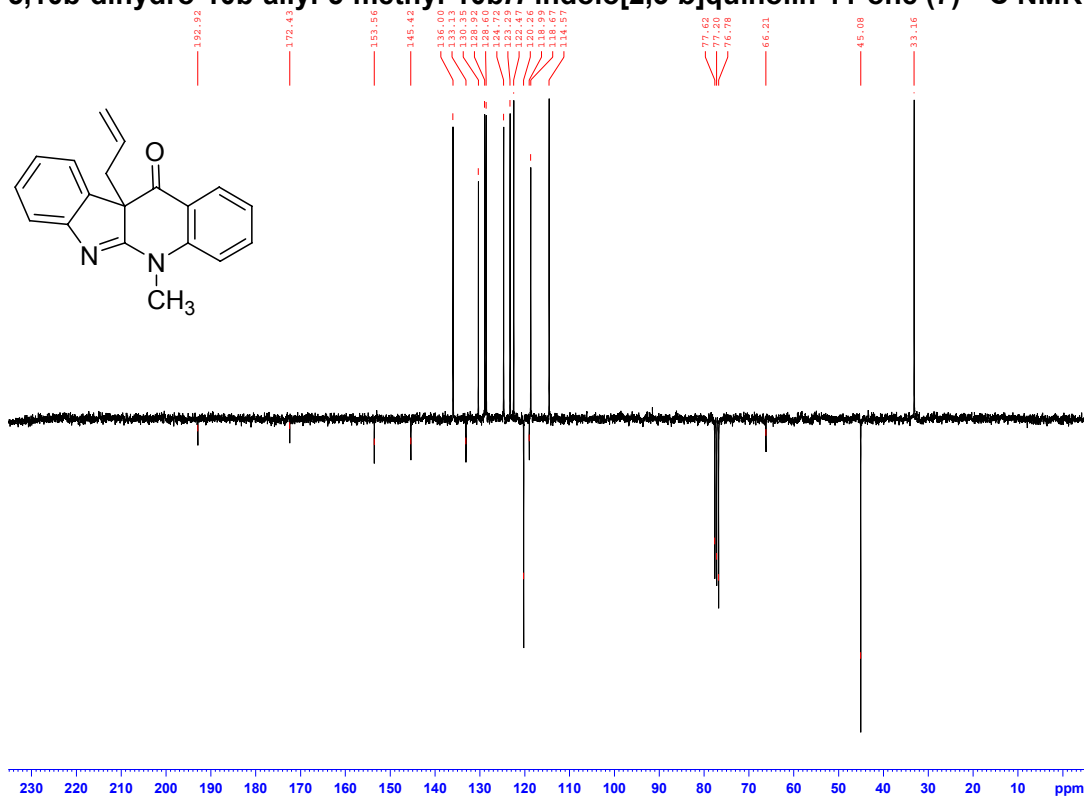


5,10b-dihydro-10b-allyl-5-methyl-10b*H*-indolo[2,3-*b*]quinolin-11-one (7) ¹H NMR in CDCl₃

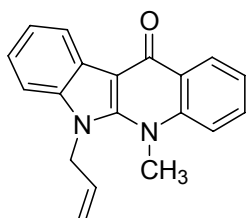
Supporting Information



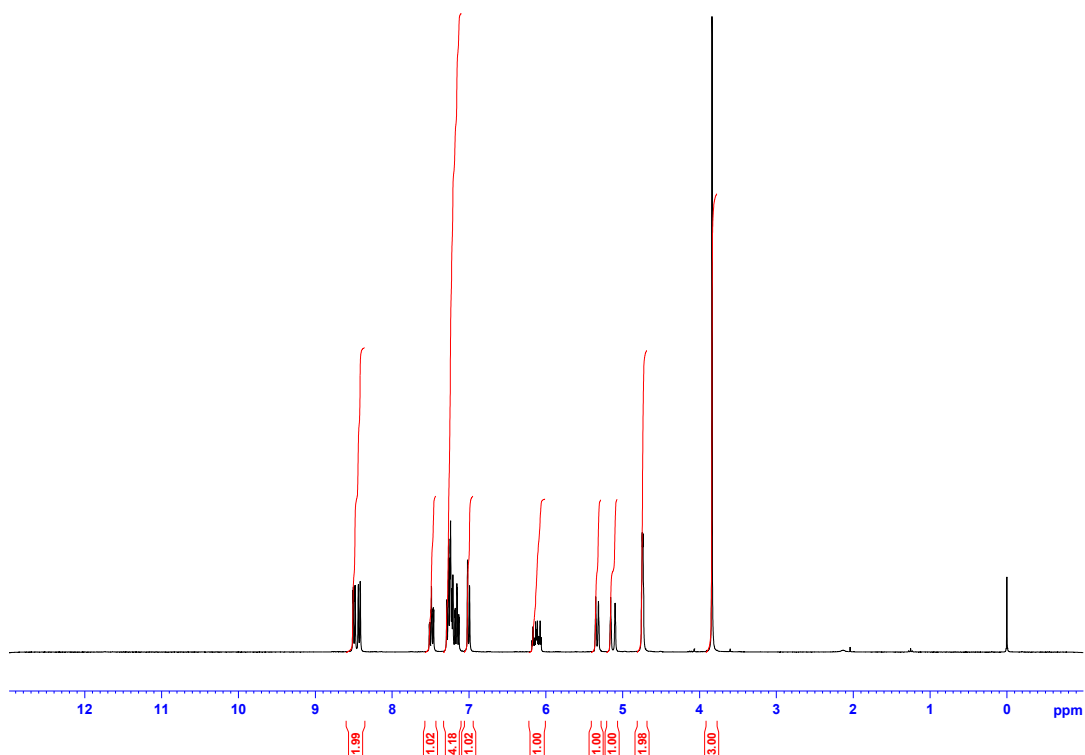
5,10b-dihydro-10b-allyl-5-methyl-10bH-indolo[2,3-b]quinolin-11-one (7) ^{13}C NMR in CDCl_3



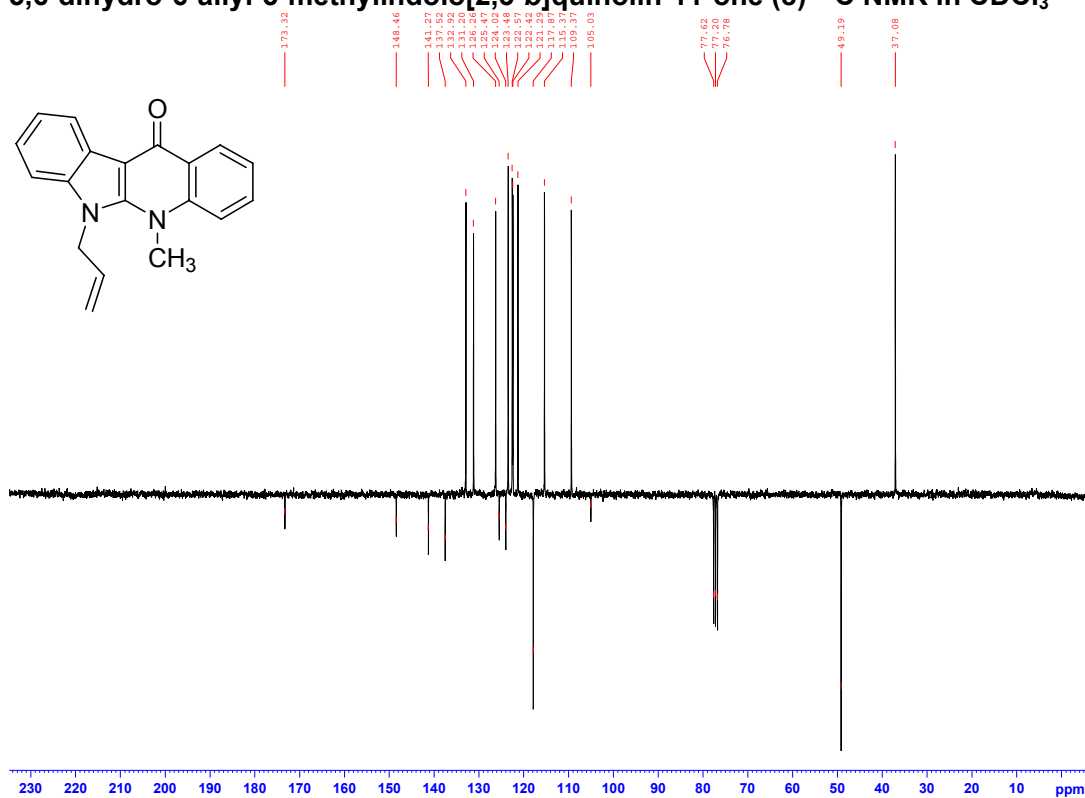
5,6-dihydro-6-allyl-5-methylindolo[2,3-b]quinolin-11-one (8) ^1H NMR in CDCl_3



Supporting Information

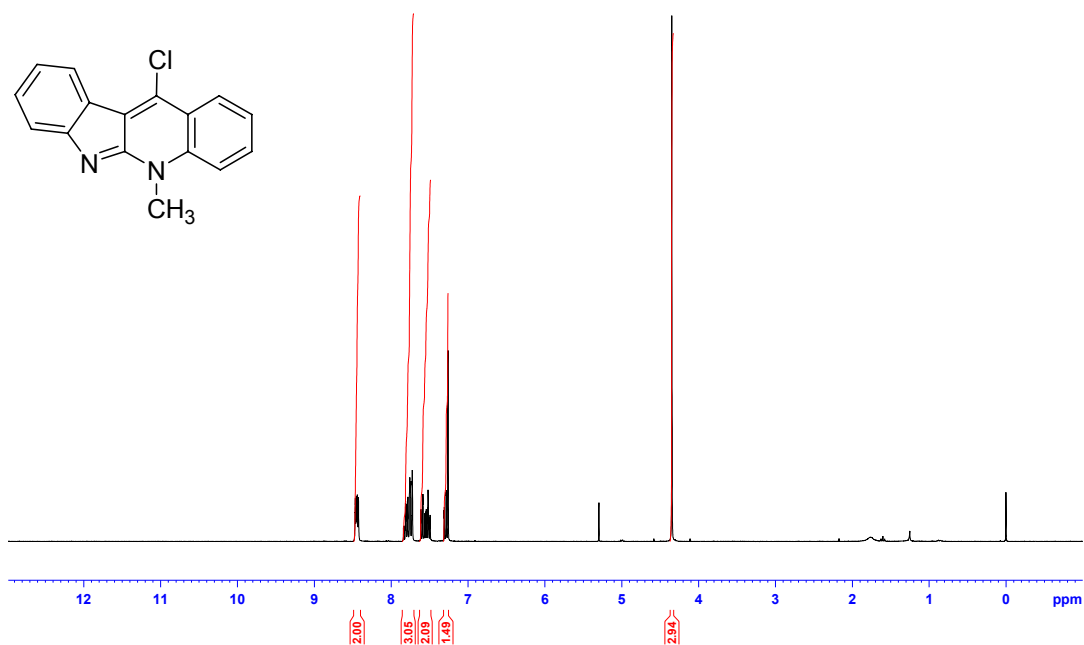


5,6-dihydro-6-allyl-5-methylindolo[2,3-b]quinolin-11-one (8) ¹³C NMR in CDCl₃

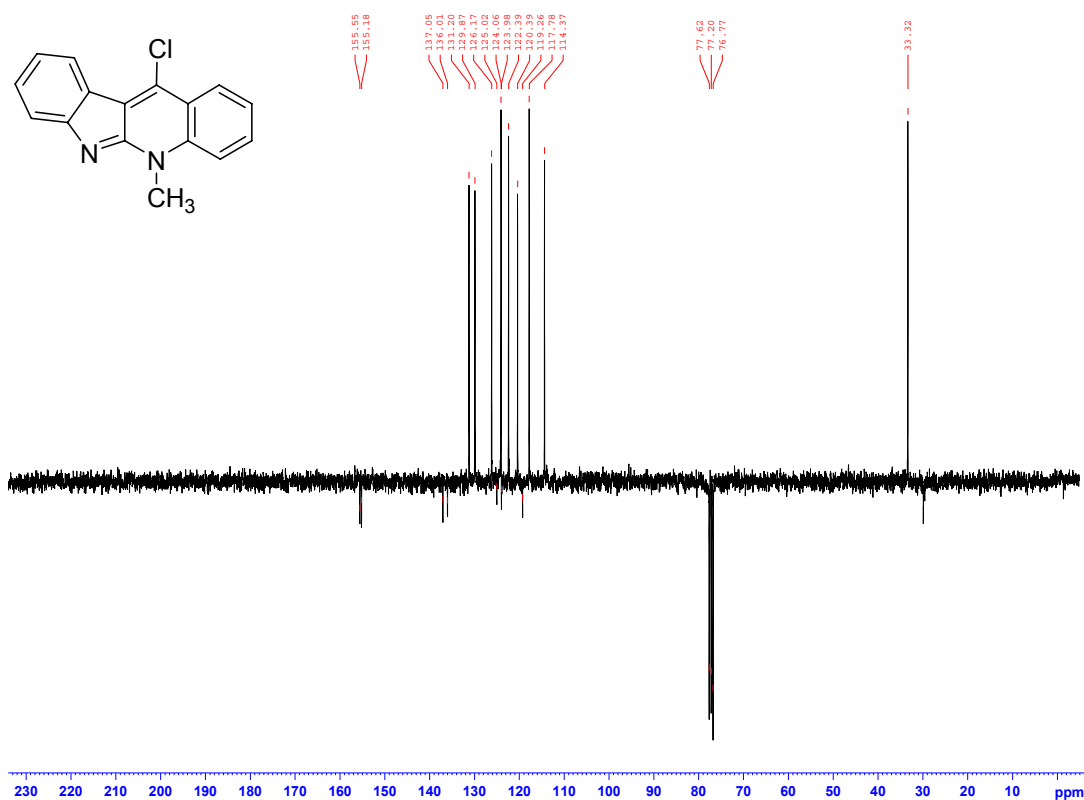


11-chloro-5-methyl-5H-indolo[2,3-b]quinoline (10) ¹H NMR in CDCl₃

Supporting Information

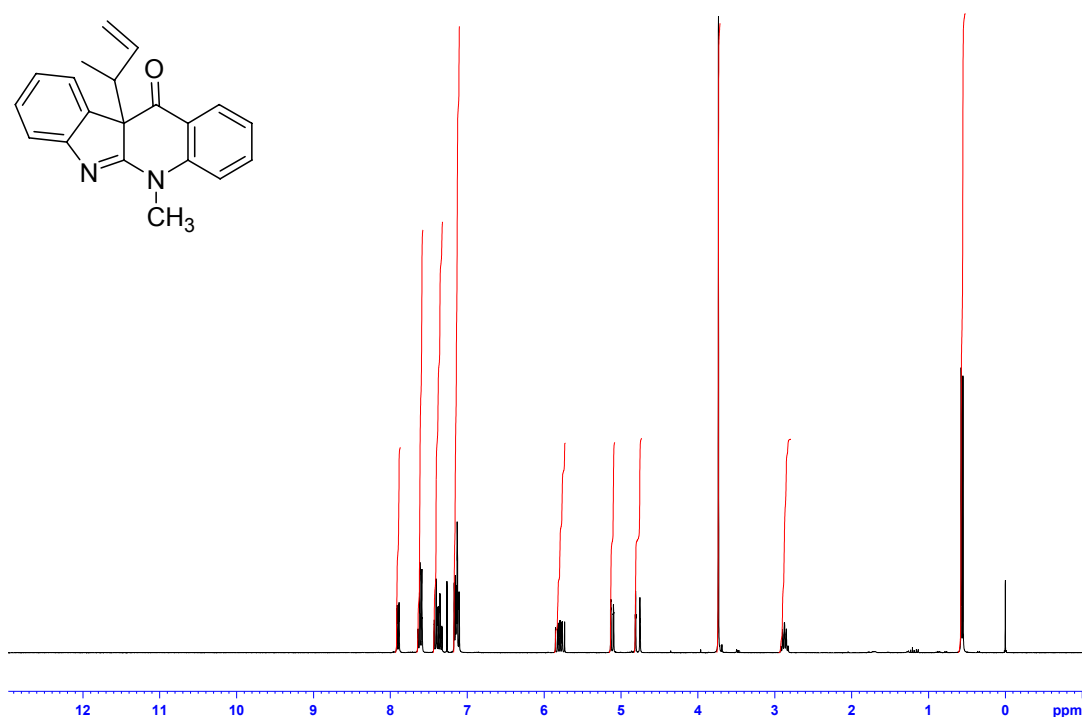


11-chloro-5-methyl-5H-indolo[2,3-b]quinoline (10) ^{13}C NMR in CDCl₃

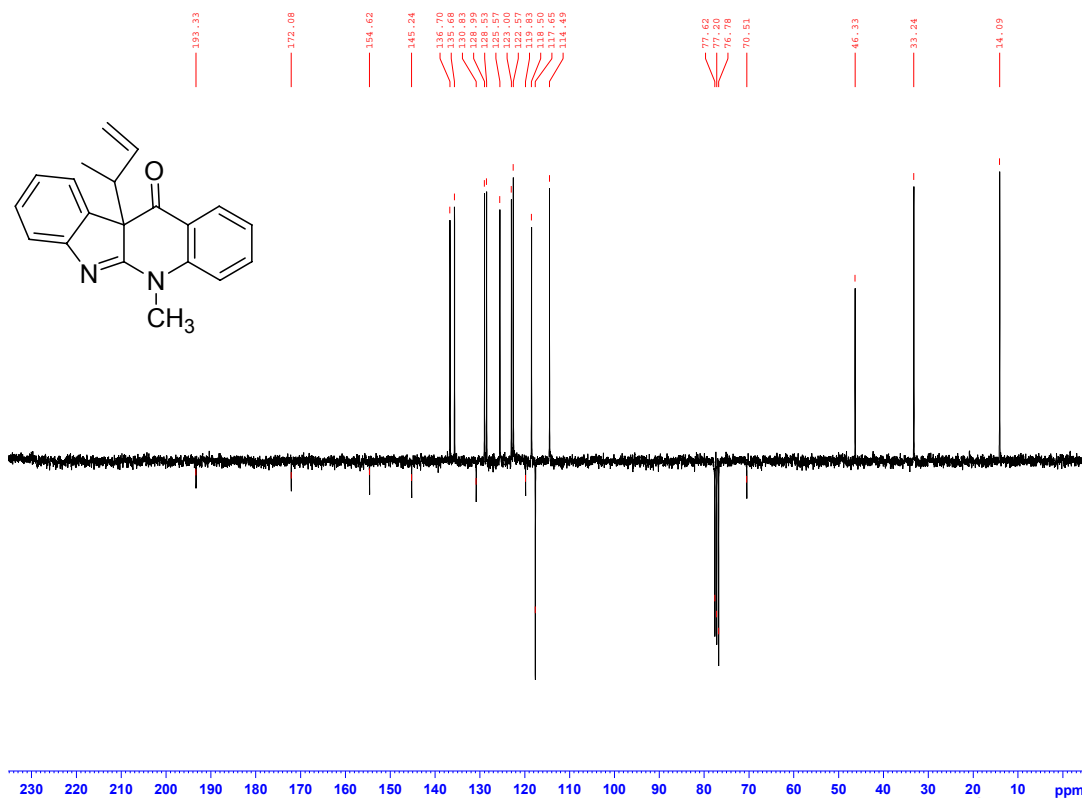


rac-(1'*R*,10*bS*)-5,10*b*-dihydro-10*b*-(1'-methylallyl)-5-methyl-10*bH*-indolo[2,3-*b*]quinolin-11-one (16a) ^1H NMR in CDCl₃

Supporting Information

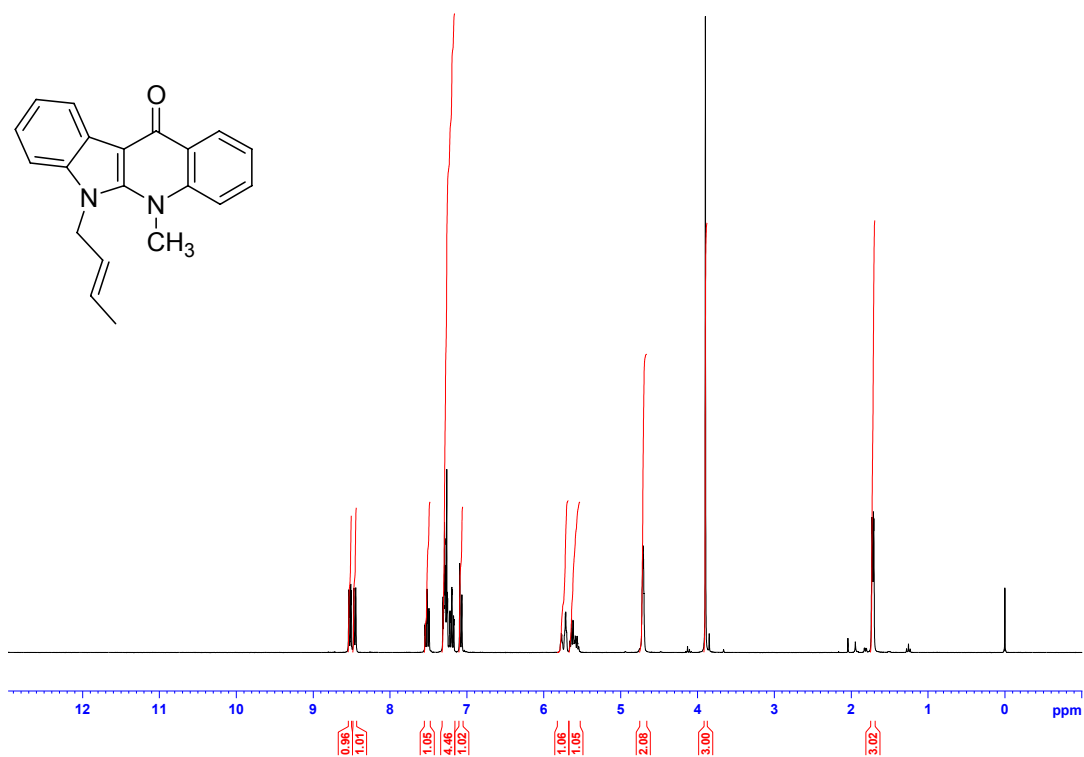


rac-(1'*R*,10*bS*)-5,10*b*-dihydro-10*b*-(1'-methylallyl)-5-methyl-10*bH*-indolo[2,3-*b*]quinolin-11-one (16a) ¹³C NMR in CDCl₃

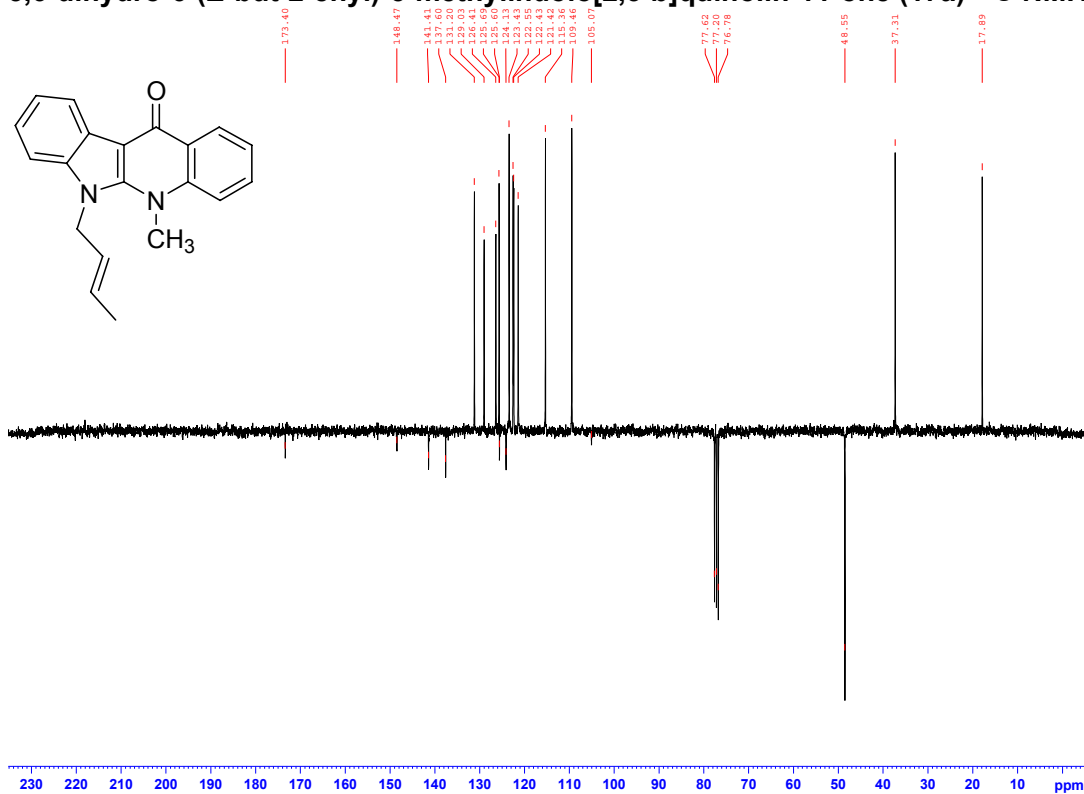


5,6-dihydro-6-(*E*-but-2-enyl)-5-methylindolo[2,3-*b*]quinolin-11-one (17a) ¹H NMR in CDCl₃

Supporting Information

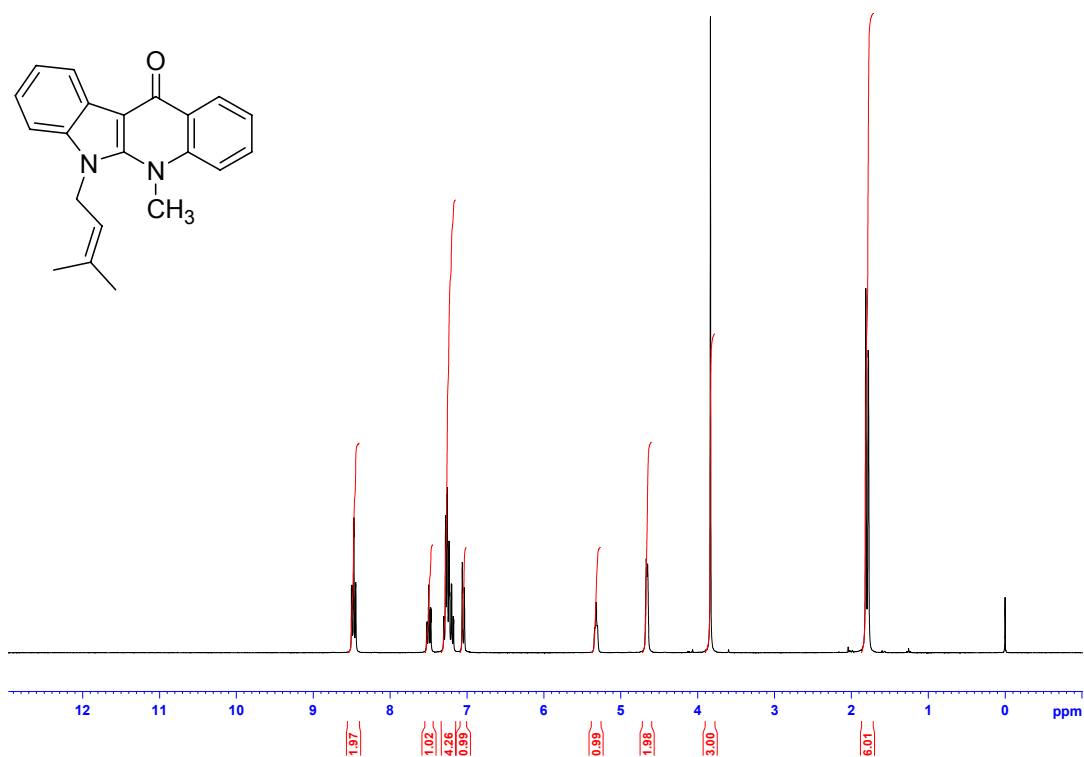


5,6-dihydro-6-(*E*-but-2-enyl)-5-methylindolo[2,3-*b*]quinolin-11-one (17a) ¹³C NMR in CDCl₃

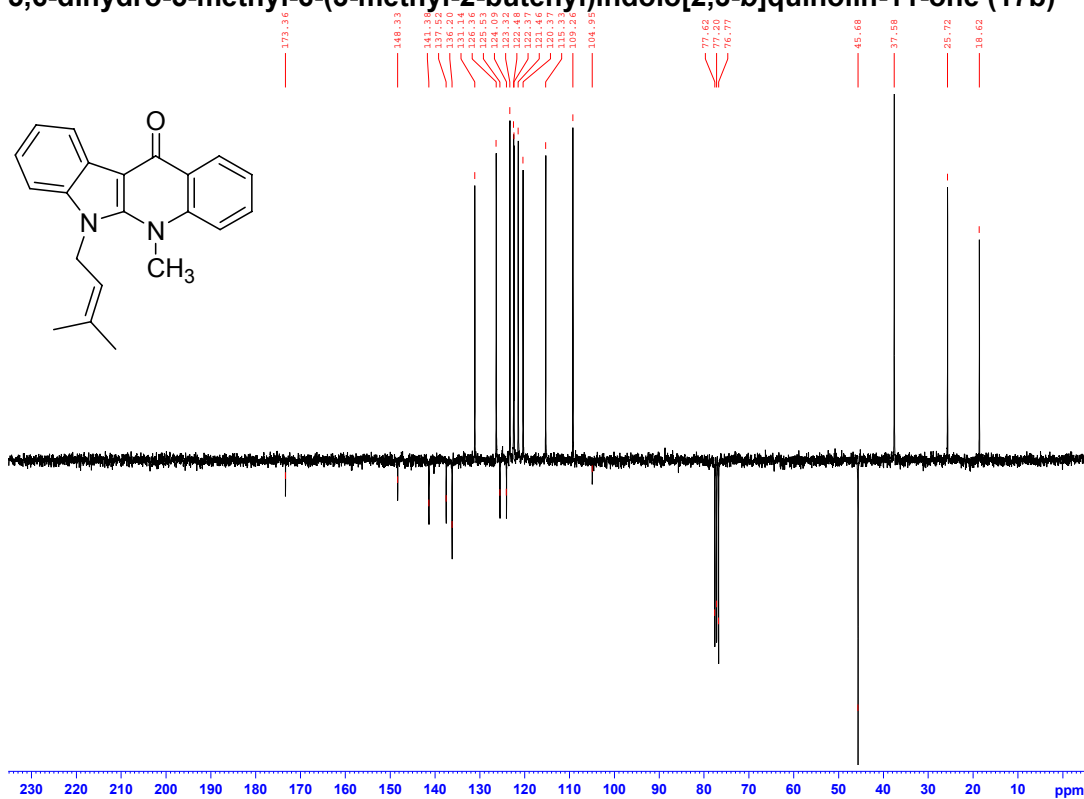


5,6-dihydro-5-methyl-6-(3-methyl-2-butenyl)indolo[2,3-*b*]quinolin-11-one (17b) ¹H NMR in CDCl₃

Supporting Information

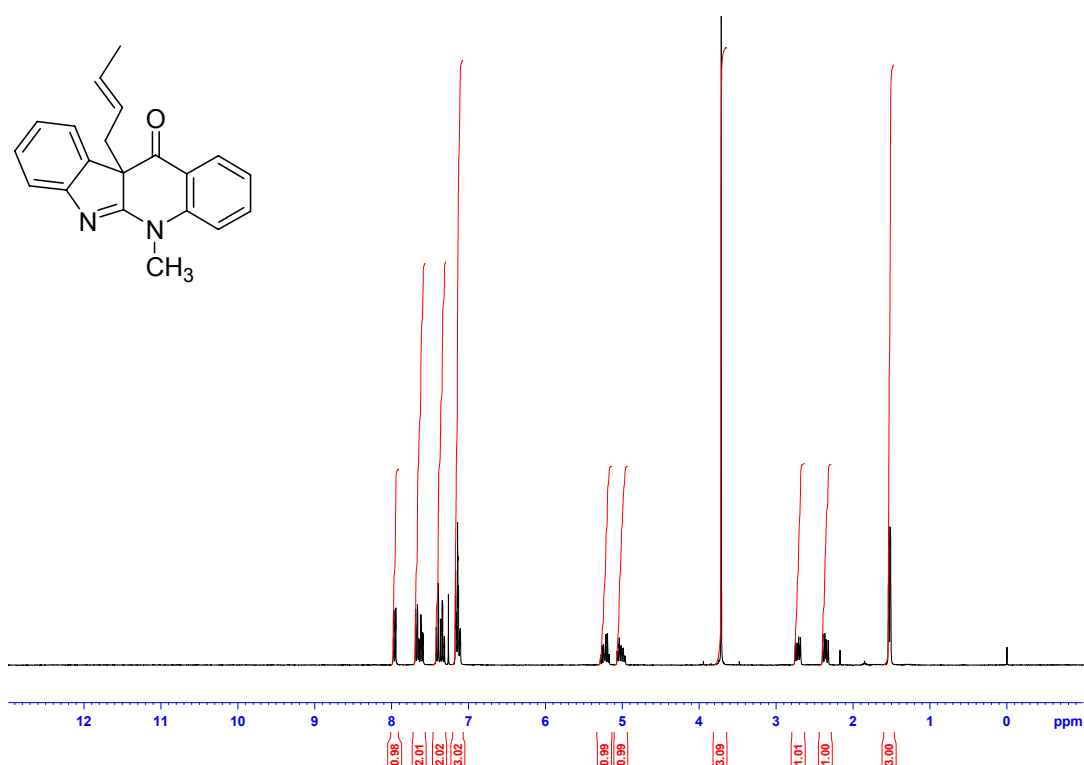


5,6-dihydro-5-methyl-6-(3-methyl-2-butenyl)indolo[2,3-*b*]quinolin-11-one (17b) ¹³C NMR in CDCl₃

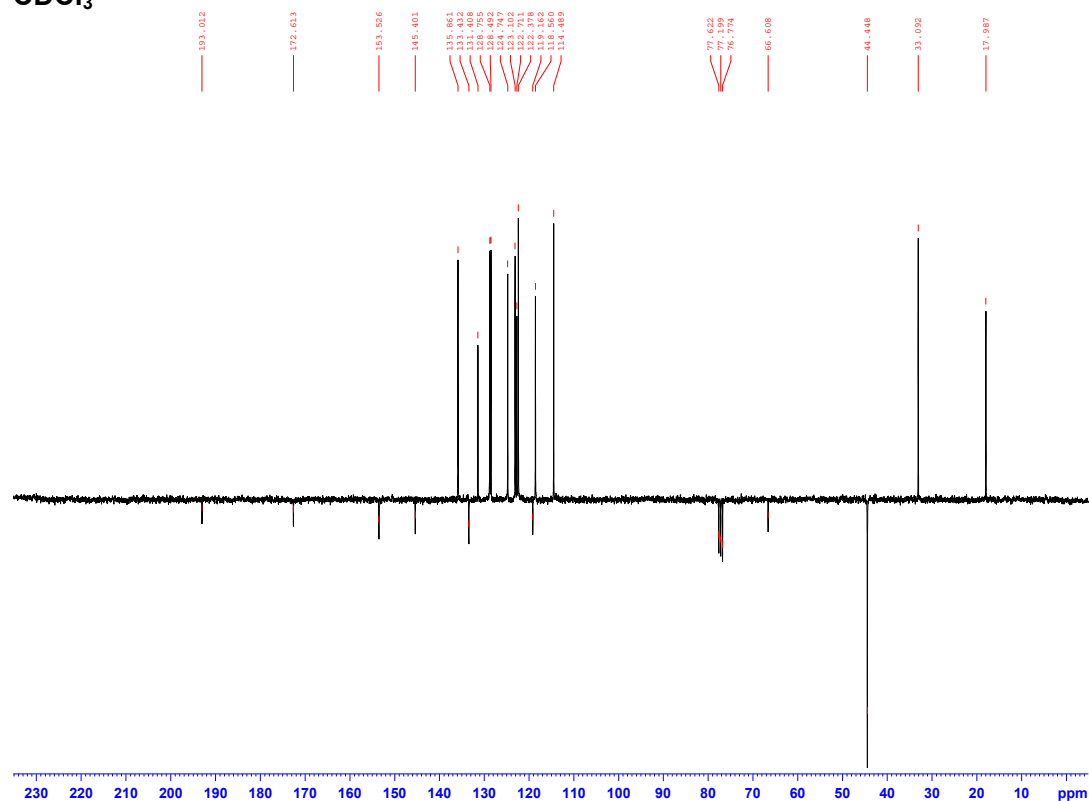


5,10b-dihydro-10b-(*E*-but-2-enyl)-5-methyl-10b*H*-indolo[2,3-*b*]quinolin-11-one (16c) ¹H NMR in CDCl₃

Supporting Information

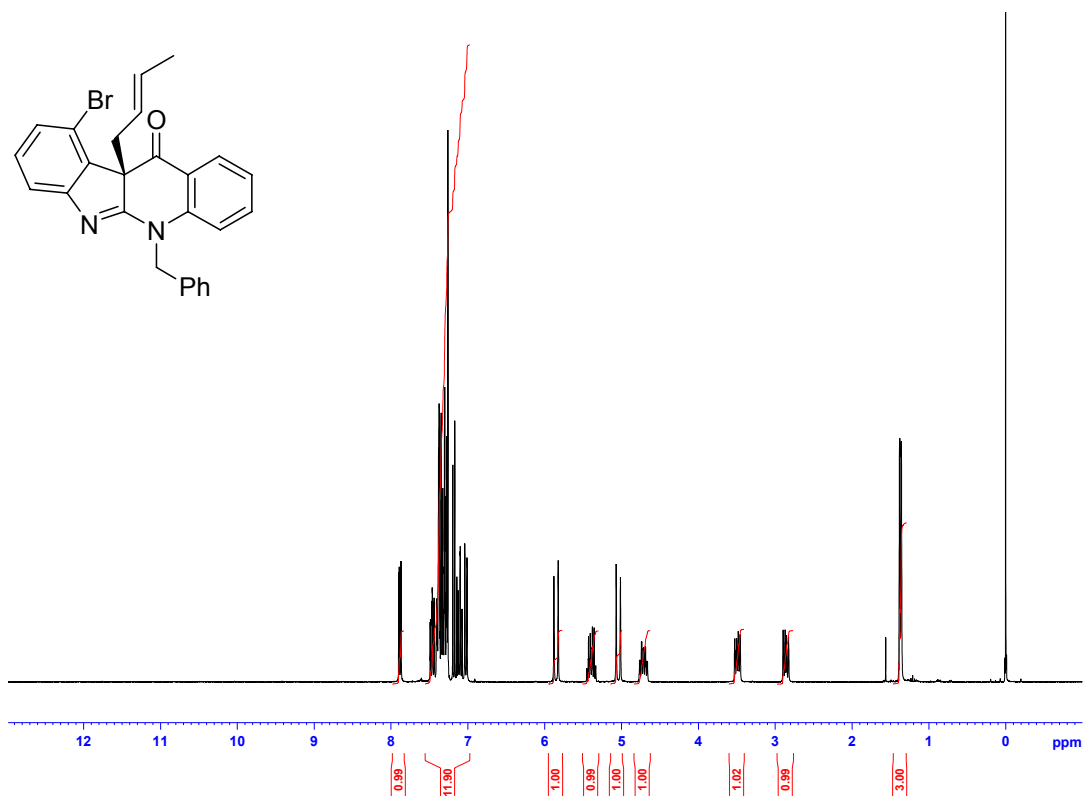


5,10b-dihydro-10b-(*E*-but-2-enyl)-5-methyl-10b*H*-indolo[2,3-*b*]quinolin-11-one (16c) ¹³C NMR in CDCl₃

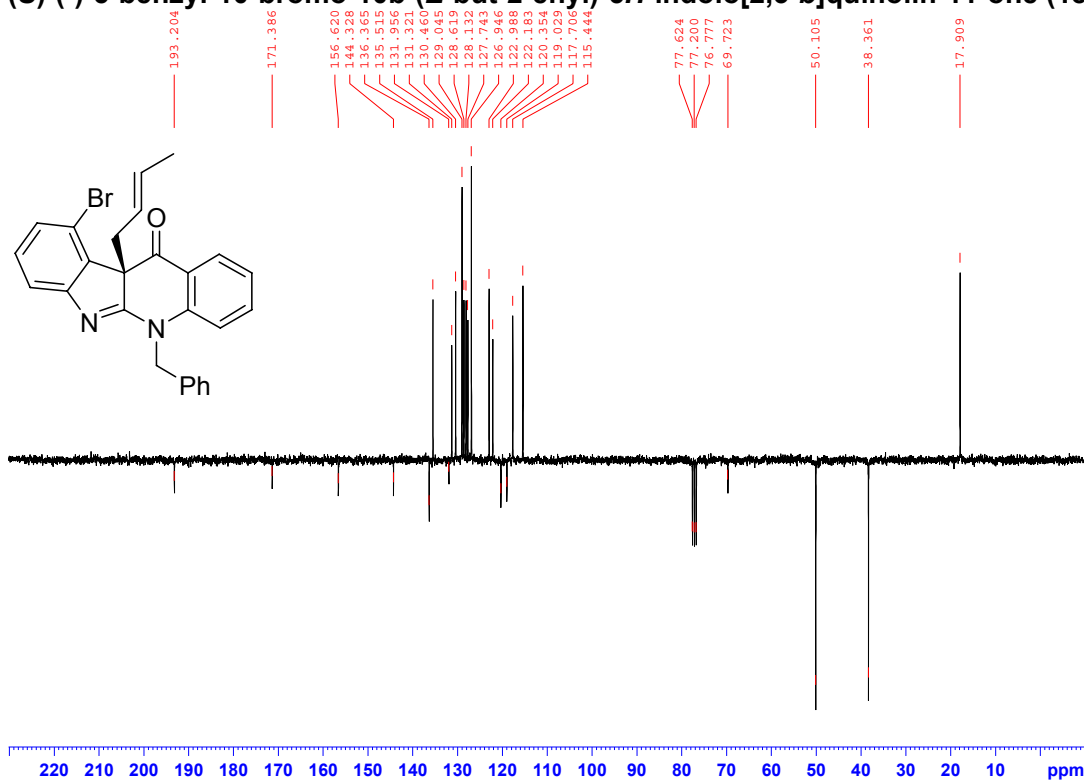


(*S*)-(-)-5-benzyl-10-bromo-10b-(*E*-but-2-enyl)-5*H*-indolo[2,3-*b*]quinolin-11-one (18) ¹H NMR in CDCl₃

Supporting Information

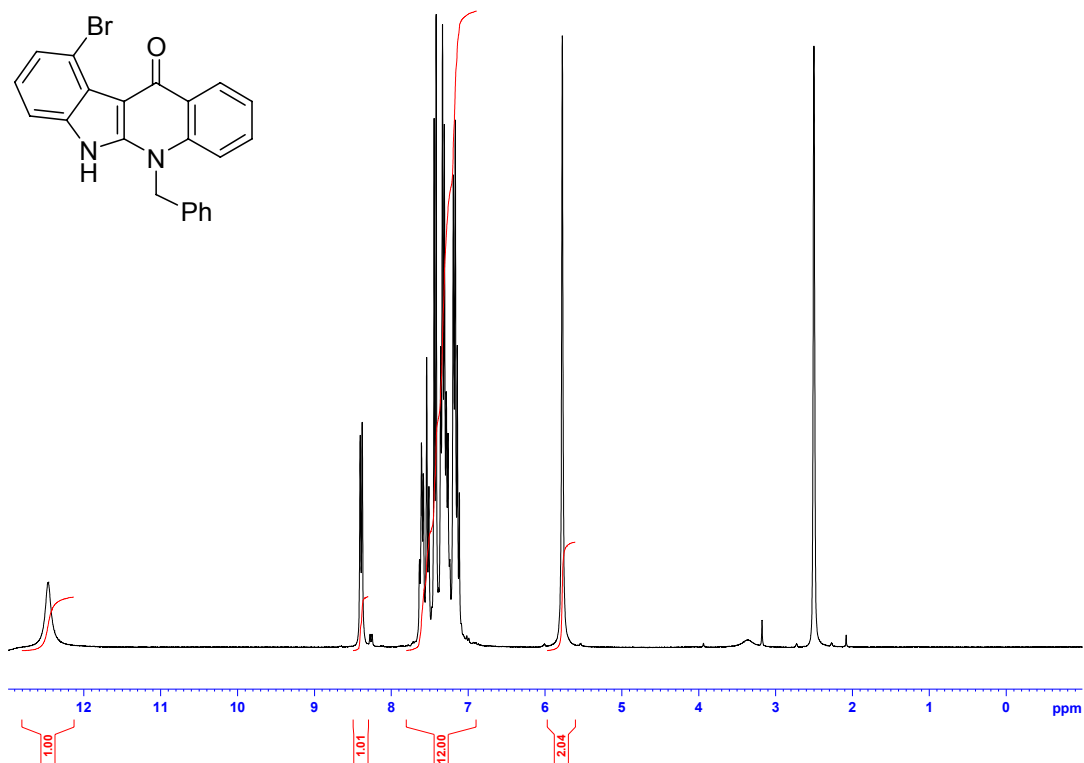


(S)-(-)-5-benzyl-10-bromo-10b-(E-but-2-enyl)-5H-indolo[2,3-b]quinolin-11-one (18) ¹³C NMR CDCl₃

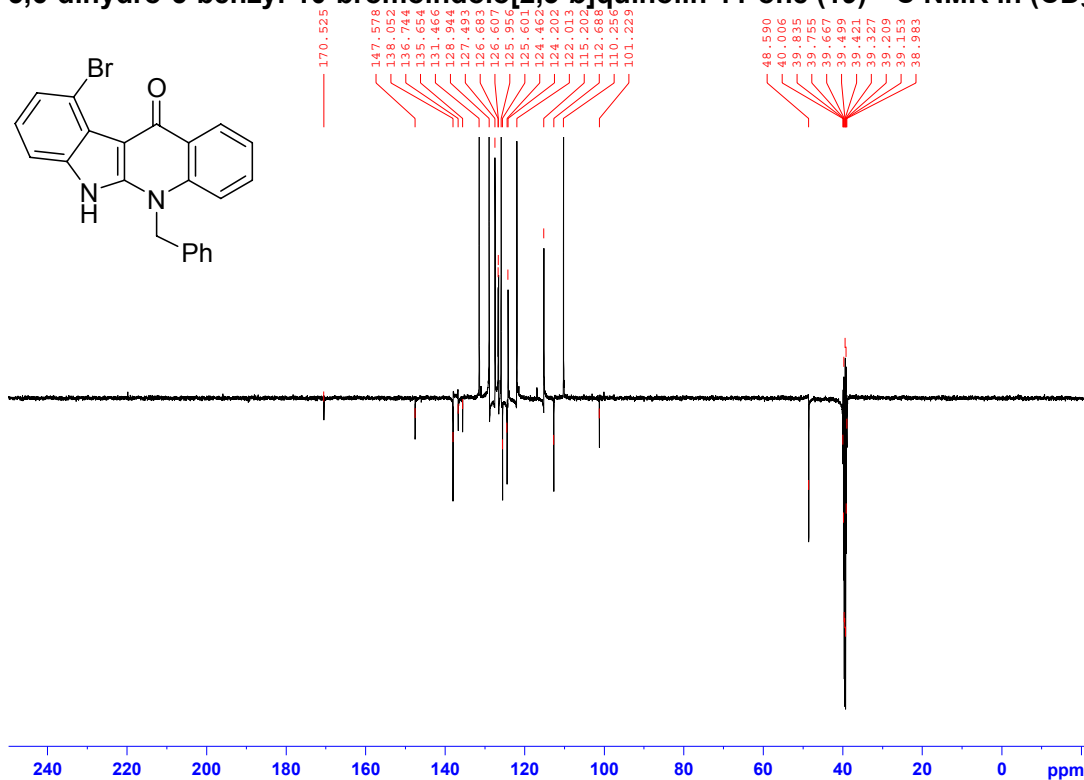


5,6-dihydro-5-benzyl-10-bromoindolo[2,3-b]quinolin-11-one (19) ¹H NMR in (CD₃)₂SO

Supporting Information



5,6-dihydro-5-benzyl-10-bromoindolo[2,3-b]quinolin-11-one (19) ¹³C NMR in (CD₃)₂SO



Supporting Information

References

- S1 MOPAC2007 J.J.P. Stewart, Stewart Computational Chemistry, Version 7.101W web:
<http://OpenMOPAC.net>
- S2 M (a) M. W. Schmidt, K. K. Baldridge, J. A. Boatz, S. T. Elbert, M. S. Gordon, J. H. Jensen, S. Koseki, N. Matsunaga, K. A. Nguyen, S. Su, T. L. Windus, M. Dupuis, J. A. Montgomery *J. Comput. Chem.* **1993**, *14*, 1347; (b) M. S. Gordon, M. W. Schmidt in *Theory and Applications of Computational Chemistry: the first forty years*, C. E. Dykstra, G. Frenking, K. S. Kim, G. E. Scuseria (Editors), Elsevier, Amsterdam, **2005**, p. 1167-1189.
- S3 Y. Gao, J.M. Klunder, R.M. Hanson, H. Masamune, S.Y. Ko and K.B. Sharpless, *J. Am. Chem. Soc.*, 1987, **109**, 5765-5780.
- S4 E. Balmer, A. Germain, W.P. Jackson, B. Lygo, *J. Chem. Soc., Perkin Trans. 1*, 1993, 399-400.
- S5 J.A. Dale, D.L. Dull and H.S. Mosher, *J. Org. Chem.*, 1969, **34**, 2543-2549.
- S6 R.R. Frazer, M.A. Petit and J.K. Saunders, *J. Chem. Soc., Chem. Commun.*, 1971, 1450-1451.
- S7 M. Somei, K. Kizu, M. Kunimoto and F. Yamada, *Chem. Pharm. Bull.*, 1985, **33**, 3696-3708.
- S8 B.S. Bal, W.E. Childers and H.W. Pinnick, *Tetrahedron*, 1981, **37**, 2091-2096.